A.R.E.A.E.E./Rep. - 233

A.R.E.A.E.E./Rep. - 233

ARAB REPUBLIC OF EGYPT

ATOMIC ENERGY ESTABLISHMENT

REACTOR & NEUTRON PHYSICS DEPARTMENT

FAST NEUTRON FLUXES DISTRIBUTION IN EGYPTIAN ILMENITE CONCRETE

By

R. M. MEGAHED, T. Z. ABOU EL-NASR

and I. I. BASHTER

1978

SCIENTIFIC INFORMATION DIVISION

ATOMIC ENERGY POST OFFICE

CAIRO, A.R.E.

We regret that some of the pages in the microfiche copy of this report may not be up to the proper legibility standards, even though the best possible copy was used for preparing the master fiche.

5,6
2,1a

A.R.E.A.E.E./Rep.- 233

ARAB REPUBLIC OF EGYPT
ATOMIC ENERGY ESTABLISHMENT
REACTOR & NEUTRON PHYSICS DEPARTMENT

FAST NEUTRON FLUXES DISTRIBUTION IN EGYPTIAN ILMENITE CONCRETE

By
R.M.MEGAHID , T.Z.ABOU EL-NASR
and I.I.BASHTER

1978
NUCLEAR INFORMATION DEPARTMENT
ATOMIC ENERGY POST OFFICE
CAIRO, A.R.E.

ABSTRACT

This work is concerned with the study of the distribution of fast neutron fluxes in a new type of heavy concrete made from Egyptian ilmenite ores.

The neutron source used was a collimated beam of reactor neutrons emitted from one of the horizontal channels of the ET-RR-1 reactor. Measurements were carried-out using phosphorus activation detectors.

Iso-flux curves were represented which give directly the shape and thickness required to attenuate the emitted fast neutron flux to a certain value. The relaxation lengths were also evaluated from the measured data for both disc monodirectional source and infinite plane monodirectional source. The obtained values were compared with that calculated using the derived values of relative number densities and microscopic removal cross-sections of the different constituents. The obtained data show that ilmenite concrete attenuates fast neutron flux more strongly than ordinary concrete. A semiemperical formula was derived to calculate the fast neutron flux at different thicknesses along the beam axis. Another semiemperical formula was also derived to calculate the fast neutron flux in ordinary concrete along the beam axis using the corresponding value in ilmenite concrete.

C O N T E N T S

INTRODUCTION

The study of radiation attenuation in concrete medii made from local material are of prime importance from the point of view of finding a new type of concrete which may prove itself a good shield for the propased nuclear power reactors. Although many theoretical methods are become available for shielding calculations, the necessity to carry out experimental measurements still remain of major importance from the point of view of providing experimental data suitable to design procedures and against which to test the theoretical calculations[1,2,3,4,5,6].

In the present work measurements were carried out to study the attenuation and flux distribution of fast neutrons in a new type of heavy concrete of density 4.6 gm/cm^3 made from the Egyptian ilmenite ore. The neutron source used for these measurements was a collimated beam of 10 cm diameter emitted from one of the horizontal channels of the ET-RR-1 reactor. The neutron flux was measured using phosphorus activation detectors.

EXPERIMENTAL DETAILS

1. Ilmenite Concretes

The concrete medium under investigation was made of Egyptian ilmenite ores mixed with steel punchings, porland cement and water. The choose of the relative constitutent of each compound in the mixure, as well as the primary mechanical tests and preparation of concrete blocks, were performed by the Institute of Building Research Center, Cairo. Special care was paid to insure homogenity and identity of the concrete medium. Table (1) gives the density of different compounds in the concrete mixure. Table(2) gives the chemical compoisition of Egyptian ilmenite ores of density 4.6 gm/cm^3. Table (3) presents the chemical composition of portland cement of density 3.15 gm/cm^3 used in the mixture. This table shows also the density of each constituent and their molecular weight. Table(4) presents the values of number densities, microscopic and corresponding macroscopic removal cross-sections for the different concrete constituents.

2. Detectors:

The detector used for fast neutron measurements was the phosphorus $^{31}P(n,p)^{31}Si$ reaction[7]. The phosphorus samples used were in the form of tablets of 4 and 2 cm diameter and 0.4 cm thick. The samples were enclosed in 0.06 cm thick cadmium cups to prevent the activation by thermal neutrons. A special holders made of aluminium and iron were designed to place the samples at the desired position in the concrete blocks as shown in Fig.(1-a). All the samples were calcibrated in the same neutron flux and a normalization coefficients were obtained. These normalization coefficients allow all the samples to achieve the same activity when placed in one and the same position in the neutron field.

3. Experimental Arrangements:

The concrete medium under investigation were shaped in the form of rectangular blocks of dimentions 120x120x40 cm (Fig. 1-b). These blocks were arranged infront of one of the horizontal channels of ET-RR-1 reactor. The blocks were placed on a large steel frame of 100 cm height, 122 cm width and 250 cm length to facilitate their adjustment and transportation. The alignment of the concrete blocks with respect to center line of the beam was carried out geometrically by adjusting the steel frame center in coincidence with that of the beam. Fig.(2) shows the geometrical arrangements of the experimental layout.

4. Experimental Errors:

The fast neutron fluxes distribution were obtained from the measured detectors activity after introducting a number of correction factors such as the sample calibration coefficients, the time factor, the efficiency of the different counting systems and normalization coefficients between different series of measurements.

An estimation of these errors has been carried out and it was found in order of $\pm$ 10%. However in some measurements where the flux is very low, the error reached $\pm$ 15%[9].

3. RESULTS AND DISCUSSIONS

The measured results of fast neutron fluxes distribution in ilmenite concrete are given in Table(5) and Figs.(3,4). Table (5) represents the value of the phosphorus detectors activities N_w at saturation for given position (R,z) which correspond in relative units to the values of fast neutron fluxes. Fig.(3) shows the fast neutron distribution along the beam direction for certain values of Z(Z = 0, 5, 10, 15 up to 85 cm). Fig.(4) shows the fast neutron fluxes distribution in a direction perpendicular to the beam direction, i.e. in the z-direction for certain values of R(R = 10, 30, 50 and 70 cm).

From Fig.(3) it can be seen that for $z = 0$ the fast neutron flux decreases exponentially with the increasing of R. For $z > 5$ cm i.e. outside the beam vicinity the flux decreases also exponentially for values of $R > 30$ cm. However for $R < 30$ cm the curves become less steeper and their stops decrease with the increasing of Z. This could be attributed to the fact that for high values of Z, the effect of scattered neutrons becomes more pronounced.

Fig.(4) shows that, for R = 10 and 30 cm, the neutron flux decreases more rapidely with the increasing of Z, for Z = 15 cm. However, for value of $Z > 15$ cm, the decrease becomes less. For R = 50 and 70 cm, the decrease in the values of neutron flux along the z-direction becomes less. This is attributed to the fact that at deep penetration the flux distribution is mainly due to scattered neutrons.

1. Iso-Flux Curves Evaluation:

To make the results given in Table (5) and Figs.(3,4) more convenient for practical calculation of the shield thickness required to attenuation the fast neutrons to certain level, use has been made from the relations given in Fig.(3) to build up the isoflux curves

presented in Fig.(5). This figure presnets the isoflux curves for a plane passing through the beam axis in the concrete shield under investigation. It gives the curves for which the flux values are preserved for fluxes differing by factor of 10. These curves show that for a collimated monodirectional neutron source, the shield thickness required to attenuate the fast neutron flux to certain level has nearly the shape of a cone with thickness nearly twice in the forward direction i.e. along the beam axis than in the side direction. This is due to the collimation of the neutron source as well as the high probability for the forward scattering.

2. Relaxation Lengths Determination:

The value of relaxation lengths were derived from the measured data of fast neutron fluxes distribution in solid ilmenite concrete given before in Table(5) and Fig.(8). The derivation was performed for disc monodirectional source, which is the actual case of the source used during these measurements, and for infinite plane monodirectional source.

2.a. Relaxation Length Evaluation for a Disc Monodirectional Source:

In this case, the activities of phosphoris detectors N_w measured at different values of R(along the beam direction) and for $Z = 0$ were plotted against R. The relation is represented in Fig.(6). This figure shows that the relation is a straight line, and the slope of which represents $\frac{1}{\lambda}$, where λ is the fast neutron relaxation length. The value of λ can be derived from the following equation:

$$\phi(R_2) = \phi(R_1)\ e^{-(R_2-R_1)/\lambda} \qquad (1)$$

where:

$\phi(R_1)$ is the fast neutron flux at distance R_1,

$\phi(R_2)$ is the fast neutron flux at distance R_2, $(R_2 > R_1)$

From equation (1), the average value of relaxation length λ has been determined by the least square fits to be: $\lambda = 6.215$ cm.

2.b. Relaxation Length Evaluation for Infinite Plane Monodirectional Source:

The transformation from disc monodirectional source to infinite plane monodirectional source was performed by integrating the activities of phosphorous detectors $N_{(w)}$ in a plane normal to the beam axis (Z-direction) for fixed R-distances. The integrated neutron flux for a plane infinite monodirectional source at a distance R, $\phi_{oo}(R)$ is given by:

$$\phi_{oo}(R) = C \int_{z=0}^{\infty} N(w)\,(R,Z)\,Z.dz \qquad (2)$$

where: C is a constant which is independent on the coordinates R and Z.

A practical evaluation of $\phi_{oo}(R)$ for different values of R were performed by determining the areas under the curves which relate $N_w\,(R,Z).Z$, versus Z for Z = 0 up to oo and for different values R. The area under these different curves were measured by the help of planemeter and the numerical values of these areas are presented in Table (6). These areas represent the flux distribution from infinite plane monodirectional source.

The relation between the integrated fast neutron flux distribution (i.e. the areas under the curves) and the distance along the R-direction is represented in Fig.(7). This figure shows that the relation is a straight line the slope of which is $1/\lambda$. Using equation (2), the average value of relaxation length (λ) has been determined by the least square fits to be:

$$\lambda = 7.589 \text{ cm.}$$

2.c. Theoretical Evaluation of Relaxation Length:

The relaxation length can be derived by calculating the total macroscopic removal cross-section $\sum_r$ of the different concrete elements. The relaxation length is given by:

$$= \frac{1}{\sum_r} \qquad \ldots\ldots\ldots\ldots\ldots\ldots \quad (3)$$

The fast neutron macroscopic removal cross-section was derived from the calculated partial number density of the different concrete constituents and the corresponding elemental microscopic removal cross-sections. The microscopic removal cross-section for these elements were taken from the data reported by Chapman et. al.[11] The values of the number densities, microscopic and corresponding macroscopic removal cross-sections for the different concrete constituents are presented in Table(4). The total macroscopic removal cross-section was calculated by adding the partial macroscopic removal cross-sections.

A value of $\sum_r = 0.1443\ cm^{-1}$ was obtained which gives the relaxation length a value, = 6.93 cm.

The calculated value of relaxation length is in reasonable agreement (within experimental error) with that values derives from experimental data obtained for both disc monodirectional source and infinite plane monodirectional source. In case of disc monodirectional source the value obtained is 10.3% lower than the calculated value, however, in case of infinite plane monodirectional source the measured value is 9.5% higher than the calculated value. This may by attributed to the fact that in case of disc monodirectional source of 10 cm diameter the probability that the scattered neutron will be removed from beam is higher. Hence the relaxation lenth is lower. However in case of infinite plane monodirectional source, all the scattered neutrons remain in the beam vicinity and hence give response to detectors activities.

3. Comparison Between Ilmenite and Ordinary Concrete:

Fig.(8) gives the fast neutron fluxes distribution along the beam direction for different values of Z for both ilmenite and ordinary concrete. The relations show that, for values of R, $R \geq 30$ cm, ilmenite concrete is better neutron attenuator than ordinary concrete. The difference in flux values increases with the increasing of R, for R = 70 cm and Z = 10 cm, the flux value is approximately 20 times less in case of ilmenite concrete. However, for values of $R < 30$ cm, the flux value in case of ordinary concrete is less than the values given for ilmenite concrete, the difference decreases with the increasing of R until the fluxes become the same at distance about 30 cm along the beam direction. This could be attributed to the fact that , for small thickness ordinary concrete attenuates fast neutron flux more rapidely. This may be due to the fact that ordinary concrete contains elements of mass number relatively less than ilmenite concrete. These elements slow down fast neutrons of lower energy by elastic collision which is more effective with elements of low mass number. However, in case of ilmenite concrete with elements of relatively high mass number such as iron and tetanium, the main process for slowing down fast neutrons of high energy (above 0.5 MeV) is by inelastic scattering. Since neutrons of higher energies could survive to some extent after deep penetration of the shield media, therefore at large values of R, along the beam direction, the main process by which neutrons of high energy could be slowed down is by inelastic scattering process. Hence at deep penetration ilmenite concrete becomes more effective for fast neutron attenuation than ordinary concrete.

An attempt was made to derive a relation between the flux values measured at Z = 0 and for different values of R for both ordinary and ilmenite concrete. The ratios between $\log \frac{\phi \text{ ordinary}}{\phi \text{ ilmenite}}$ were plotted

against R and is given in Fig.(9). This figure shows that the relation is a straight line with increasing values as R increases. From this relation the following semi-emperical formula was obtained which gives the values of fast neutron flux in any one of these concretes if its corresponding values is known in the other.

$$\phi_{or} = \phi_{il}\ e^{(0.0242R - 0.22)} \quad \ldots\ldots\ldots\ldots\ldots\ldots$$

using this relation the fast neutron flux was calculated along the beam direction at Z = 0 for both ordinary and ilmenite concrete and a good agreement was observed between the calculated and measured values.

CONCLUSIONS

The measured data obtained for fast neutron fluxes distributions in Egyptian ilmenite concrete gives the following conclusions:

(1) The comparison between data measured in ordinary and ilmenite concrete show that ilmenite concrete is much better for fast neutron attenuation than ordinary concrete especially for large thickness. However for small thickness i.e. less than 30 cm ordinary concrete is the best.

(2) At the beginning of neutron penetration in ilmenite concrete, the thickness required to attenuate the flux to certain value along the beam direction is approximately twice the thickness required to attenuate the flux to the same value along the perpendicular direction. However for large penetration, the thickness required to attenuate the flux to a certain value is approximately the same for all direction.

(3) The observed difference between the derived values of relaxation lengths for disc monodirectional source and plane monodirectional source could be attributed to the fact that, in case of disc monodirectional source or a collimated beam of fast neutrons the spatial distribution along the beam direction is mainly due to unscattered neutrons.

A C K N O W L E D G E M E N T S

The authors are grateful to Pref. Dr. I. Hameuda, Vice Chairman of the A.E.E., Cairo., for his interest. They are also grateful to the members of the shielding group and to the reactor personel for fruitful ceoperation. The members of the Bulding Research Center Cairo, especially Pref. Y. M. Yousseef should also be acknowledge for the preparation of concrete mixture and blocks.

REFERENCES

(1) H.Coldstein, "Principle of Reactor Shielding" Addison-wesley Publishing Co. London, (1959).

(2) B. Price et al., "Radiation Shielding" Pergamon Press, London, (1957).

(3) S. Glasstone, "Principles of Nuclear Reactor Engineering" Mac-Millan & Co. Ltd., London, (1955).

(4) J. Lamarsh, "Introduction to Nuclear Reactor Theory" Addison-Wesley Publishing Co. London, (1966).

(5) S.Glasstone and M.C. Edlund, "The Element of Nuclear Reactor Th Theory" Mac-Millan & Co. Ltd., London, (1952).

(6) Proceeding of the conference of the Physics Problems of Reactor Shielding" Held at the Atomic Energy Research Establishment, Harwell, Vol. 1,2,3,4 and 5, (1967).

(7) W.Prince, "Nuclear Radiation Detection" McGraw-Hill Book Co. Inc., New York, (1958).

(8) R.Megahid, et al. "The effect of cylindrical air filled ducts in water on the distribution of thermal and fast neutrons from a collimated beam, A.E.E., Rep. 26, A.E.E. (1966).

(9) I.I. Bashter, "Measurement of the effect of the cylindrical air filled ducts on the distribution of fast neutrons flux im the Egyptiam ilmenite concrete" M. sc. Thes is, Physics Dept. Al-Azher University, Cairo, A.R.E. (1978).

(10) M. Abd-El-Razek et al., "The effect of cylindrical air filled ducts on the distribution of fast neutrons in ordinary concrete". A.E.E., Rep-42, ARE, (1967).

(11) G. Chapman, et al., "Effective Neutron Removal Cross-Sections for shilding". USAEC Report AECD-3978, Oak Ridge National Laboratory, (1955).

Table (1)

Composition of Ilmenite Concret, Density 4.6 gm/cm^3.

Material	Composition		
	Wt%	vol %	Density gm/cm^3
Ilmenite Coarse aggregate "a"	18.09	18.4	4.72
Ilmenite Fine aggregate "b"	18.41	18.72	4.72
Steel punchings	50.7	30.92	7.87
Portland cement	9	13.72	3.15
Water	3.8	18.24	1.0

a) Coarse aggregate specifications:

16.49 per cent of grain size vary from 3/4 "to $1\frac{1}{2}$" ,
26.31 " " " " " " 3/8 "to $\frac{3}{4}$" ,
57.19 " " " " " " 3/16 to 3/8",

b) Fine aggregate specifications :

29.482 per cent of grain sizes vary from 3/32 "to 3/16",
29.310 " " " " " " 3/64 "to 3/32",
15.698 " " " " " " 3/128"to 3/64",
13.793 " " " " " " 3/256"to 3/128
11.724 " " " " " " 3/512"to 3/256",

Table (2)

Chemical Composition of Egyptian Ilmenite, Density 4.72 gm/cm^3

Material	Composition		Density gm/cm^3	Mol.wt.
	wt %	Vol %		
TiO_2	44.76	65.22	4.248	79.90
FeO	30.12	32.71	5.7	71.85
Fe_2O_3	23.16	0.27	5.24	159.69
MnO	1.29	1.46	5.44	70.94
CrO_3	0.14	0.16	5.21	151.99
V_2O_5	0.084	0.15	3.357	181.88

Table (3)

Chemical Composition of Portland Cement, Density 3.15 gm/cm^3.

Material	Composition		Density	Mol. wt.
	wt %	Vol %	gm/cm^3	
CaO	56.5	63.3	3.32	56.08
SiO_2	22.0	26.72	2.64	60.08
Al_2O_3	2.26	5.04	3.97	101.96
Fe_2O_3	3.25	1.99	5.25	159.60
MgO	2.5	2.25	3.58	40.31
SO_3	0.5	0.70	2.29	80.06

Table (4)

Atomic Densities and Microscopic Removal Cross-Section of Various Elements in Ilmenite Concrete.

Element	Atomic density $N_D, 10^{24}$ atoms/cm^2	r barns	Σ_r cm^{-1}
Ti	0.00522	1.77	0.009239
Fe	0.05134	1.98	0.101653
O	0.02627	0.99	0.026007
Mn	0.00022	1.93	0.000425
Cr	0.00003	1.87	0.000056
V	0.000007	....	.....
Ca	0.0020	1.58	0.003160
Si	0.00055	1.26	0.000693
Al	0.00033	1.31	0.000432
Mg	0.0001	1.22	0.000122
H	0.0025	1.00	0.00250
Total			0.144287

Table (5)

Fast Neutron Flux Distribution in soild Ilmenite Concrete

Z(cm) / R(cm)	0	5	10	15	20	25	30	35
10	3.81×10^{4}	2.09×10^{4}	7.287×10^{3}	2.312×10^{3}	8.17×10^{2}	3.65×10^{2}	2.01×10^{2}	1.15×10^{2}
30	2.257×10^{3}	1.45×10^{3}	6.94×10^{2}	3.32×10^{2}	2.02×10^{2}	1.23×10^{2}	8.4×10^{1}	6.1×10^{1}
50	7.4×10^{1}	5.2×10^{1}	3.9×10^{1}	2.1×10^{1}	1.4×10^{1}	1.1×10^{1}	9	7.3
70	2.6	1.74	1.21	---	---	---	---	---

Table (6)

Distribution of Fast Neutron Flux From Plane Mono-directional Source, in Solid Ilmenite Concrete.

R, cm.	Areas under the curves relating N_w (R,Z).Z versus Z.	Log. (Area)
10	1.32×10^6	6.12
30	1.72×10^5	5.235
50	1.10×10^4	4.041
70	5.0×10^2	2.699

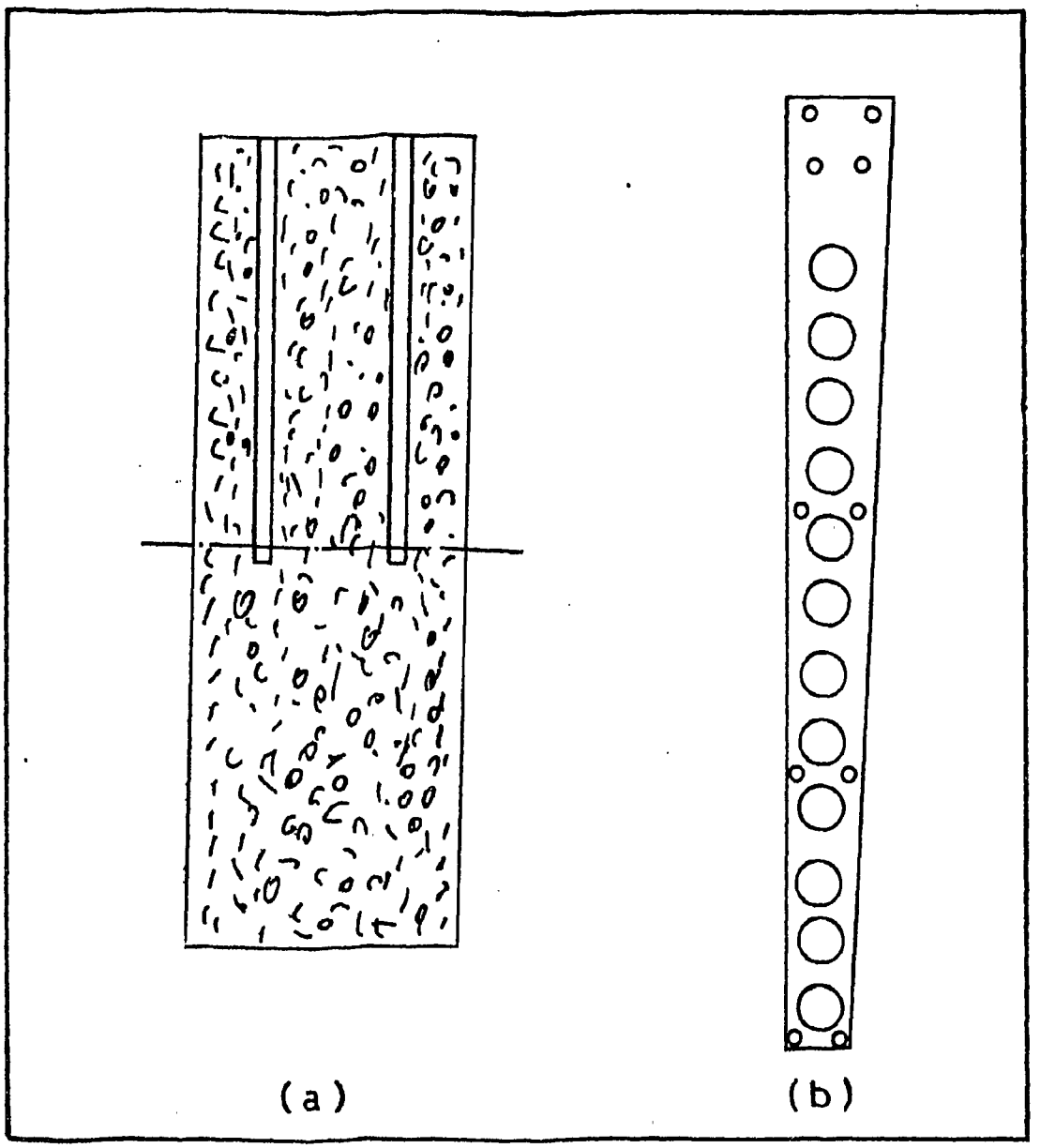

Fig.(1): a - Vertical cross section in the concrete blocks.
b - Sample holder.

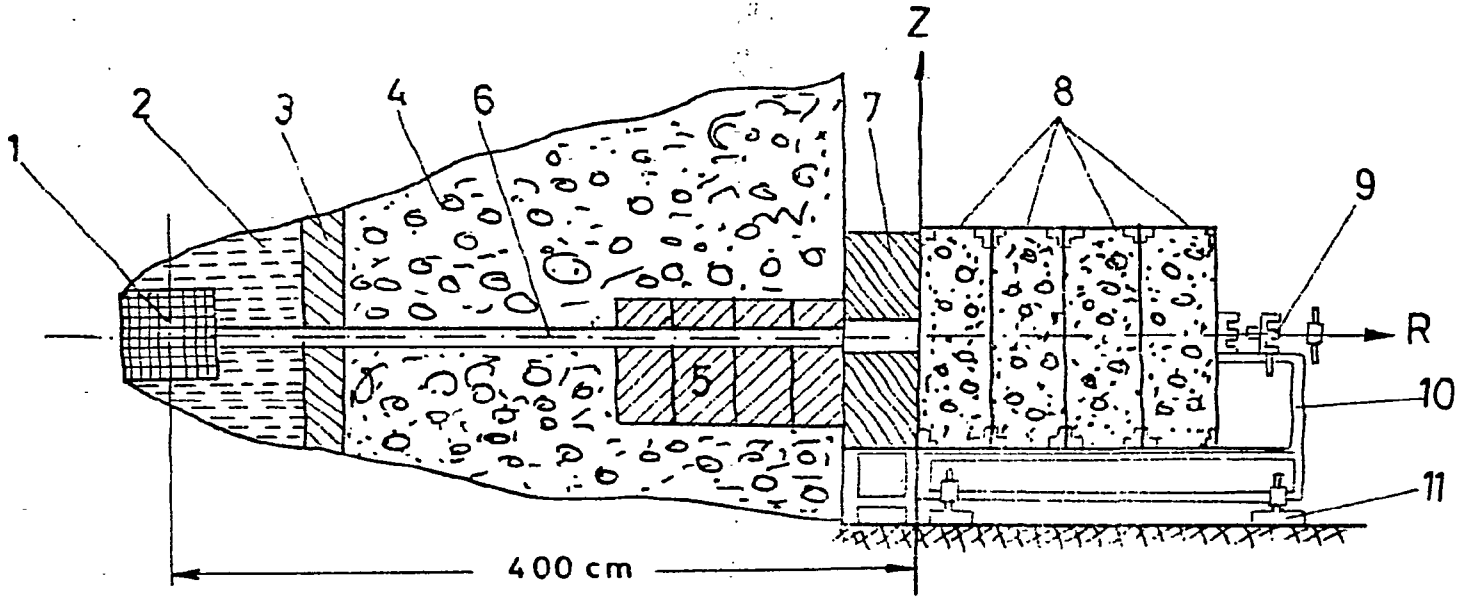

Fig.(2): The schematic diagram of the experimental layout:

1- Reactor core.
2 - Water cooling.
3- Cast-iron wall.
4 - Concrete wall surrounding the reactor
5- Cast-iron shielding-gap with concrete aggregate.
6- Experimental channel
8- Investigated ilmenite concrete blocks.
7- Coolimator.
9- Bolt system
10- Casstte bed.
11 Regulators of the cassette height.

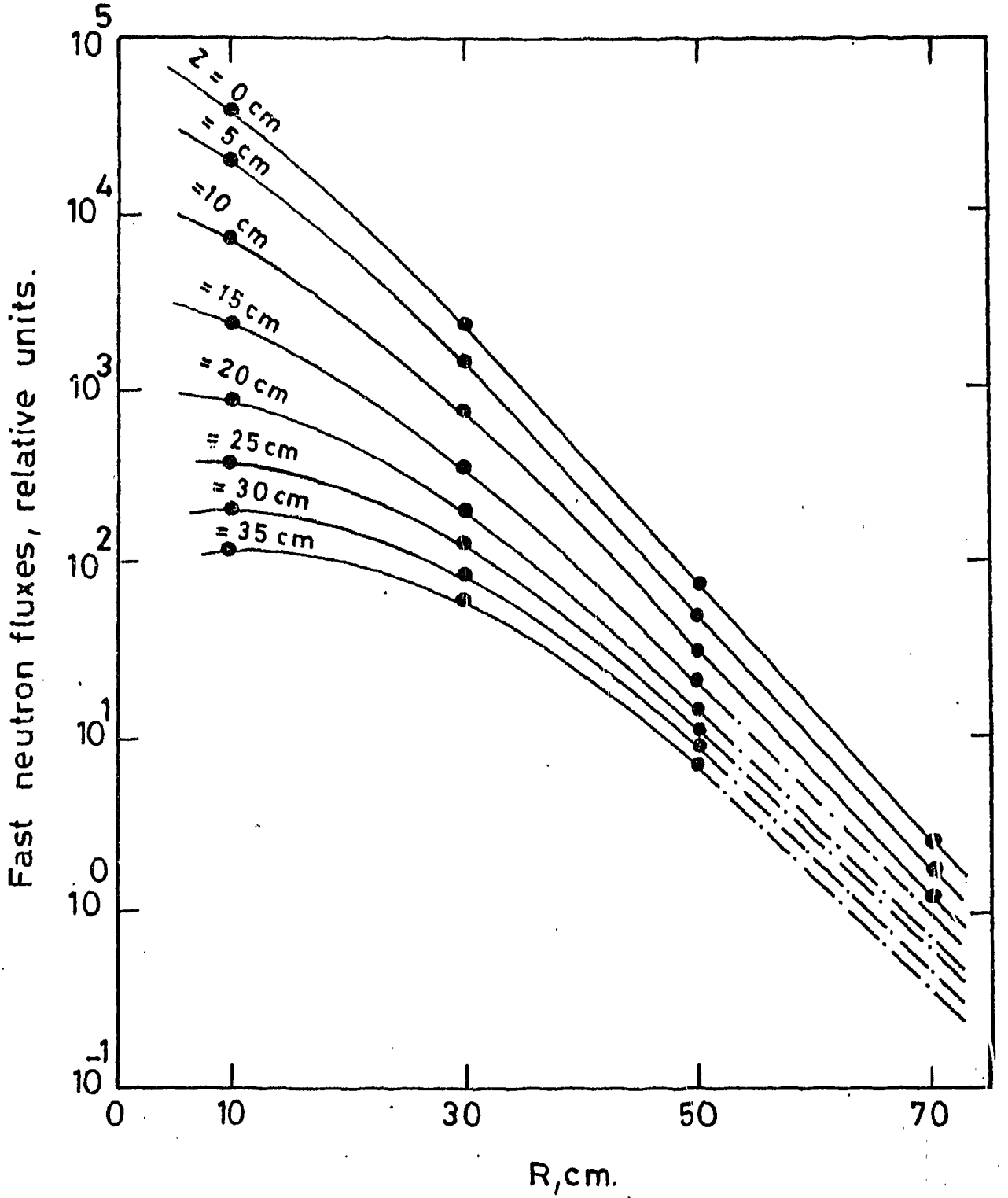

Fig.(3): Fast neutron fluxes distribution in homogenous Egyption ilmenite concrete a long a direction parallel to the beam.

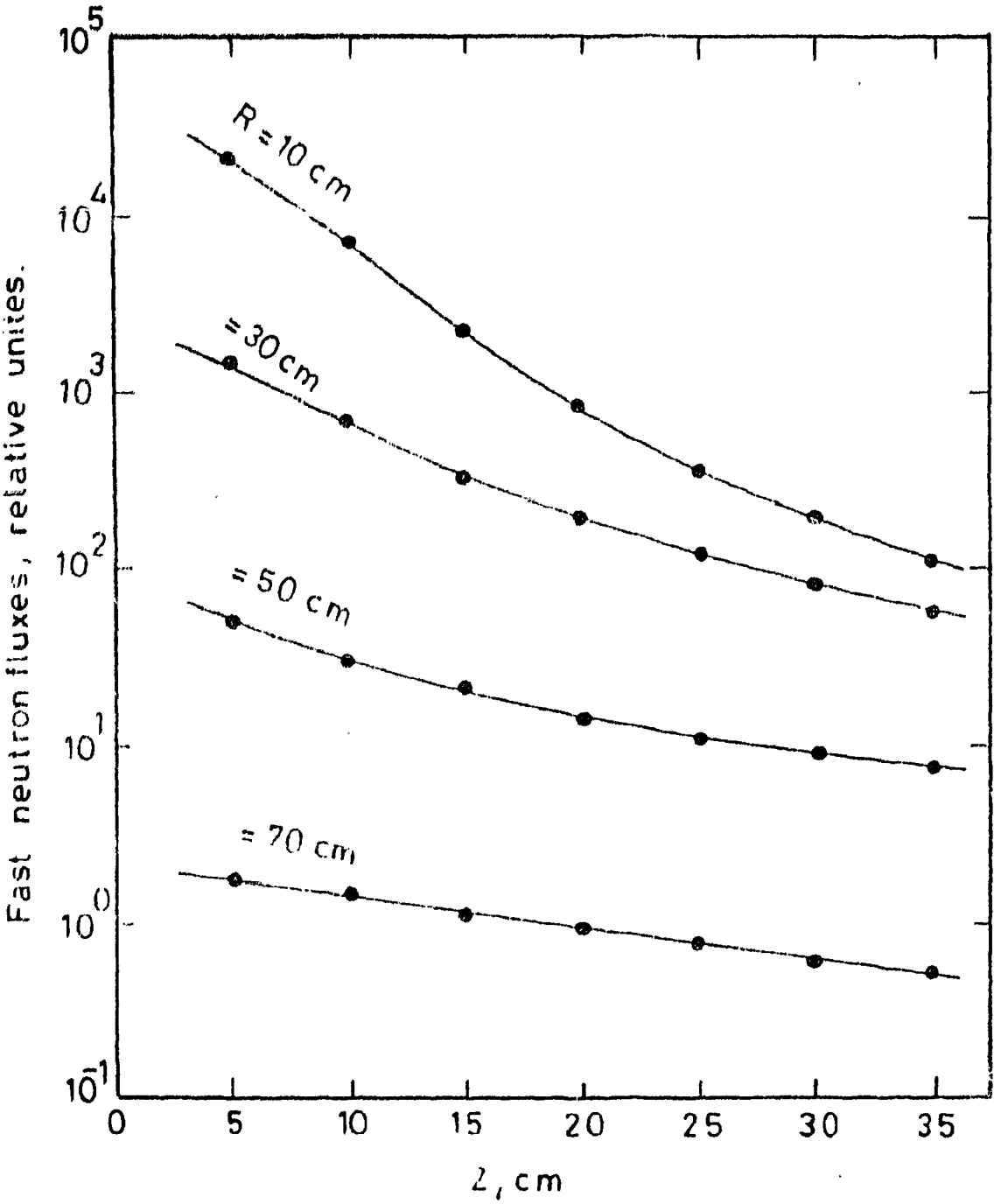

Fig.(4): Fast neutron fluxes distribution in solid concrete a long a direction perpendicular to the beam.

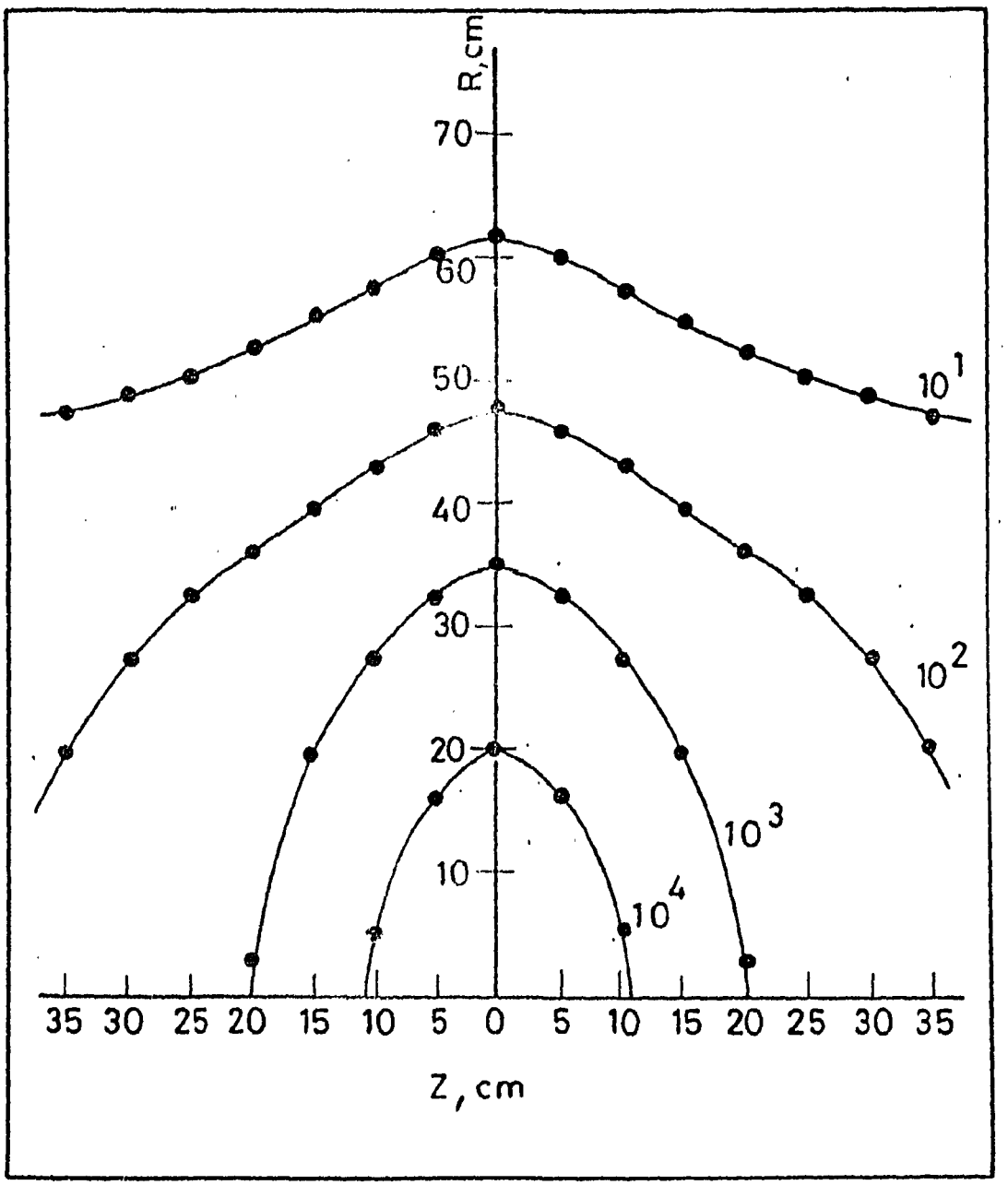

Fig.(5):Isoflux curves for fast neutrons distribution in solid concrete .

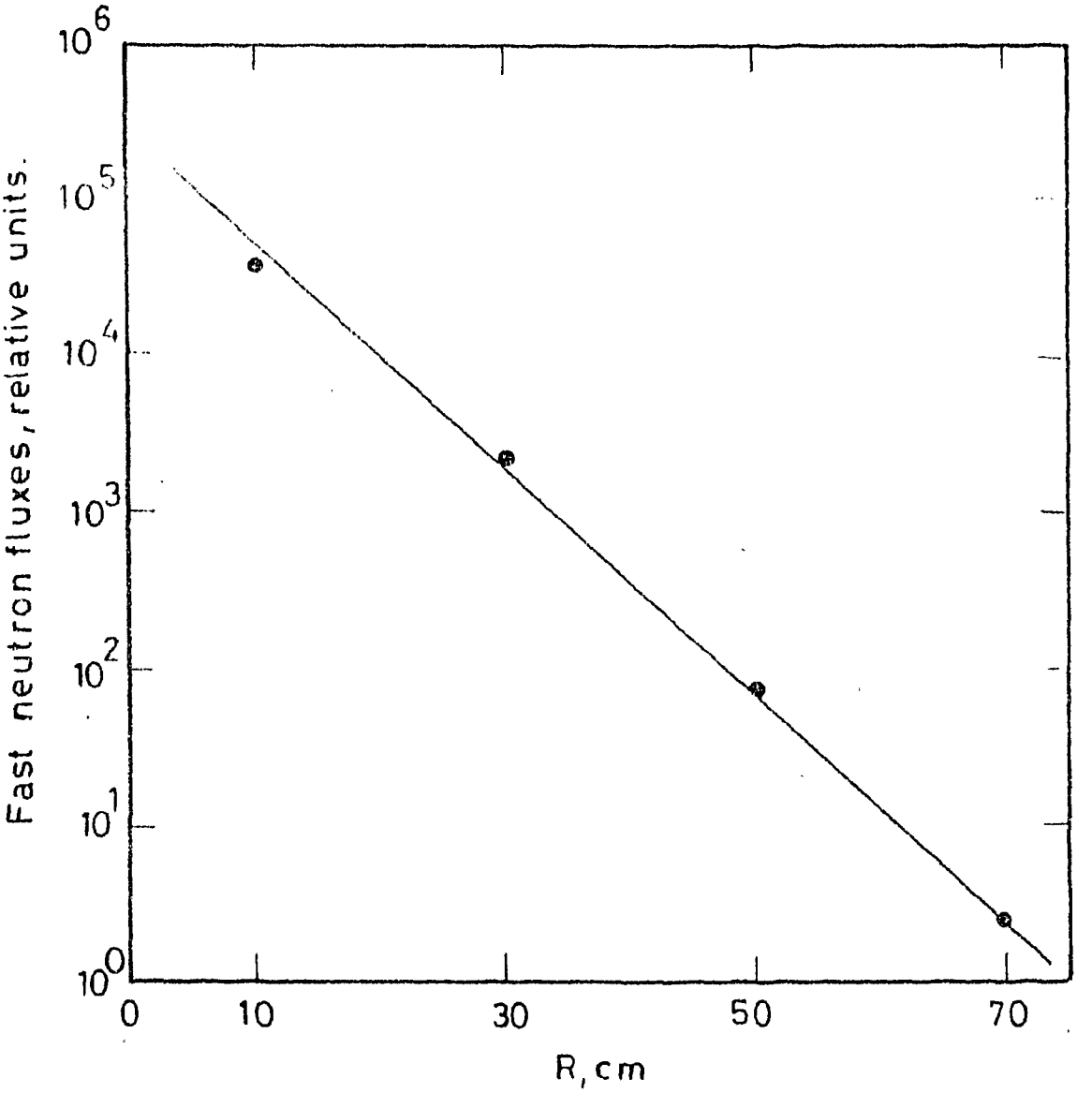

Fig.(6): Fast neutron fluxes distribution a long the beam direction for Z=0 cm .

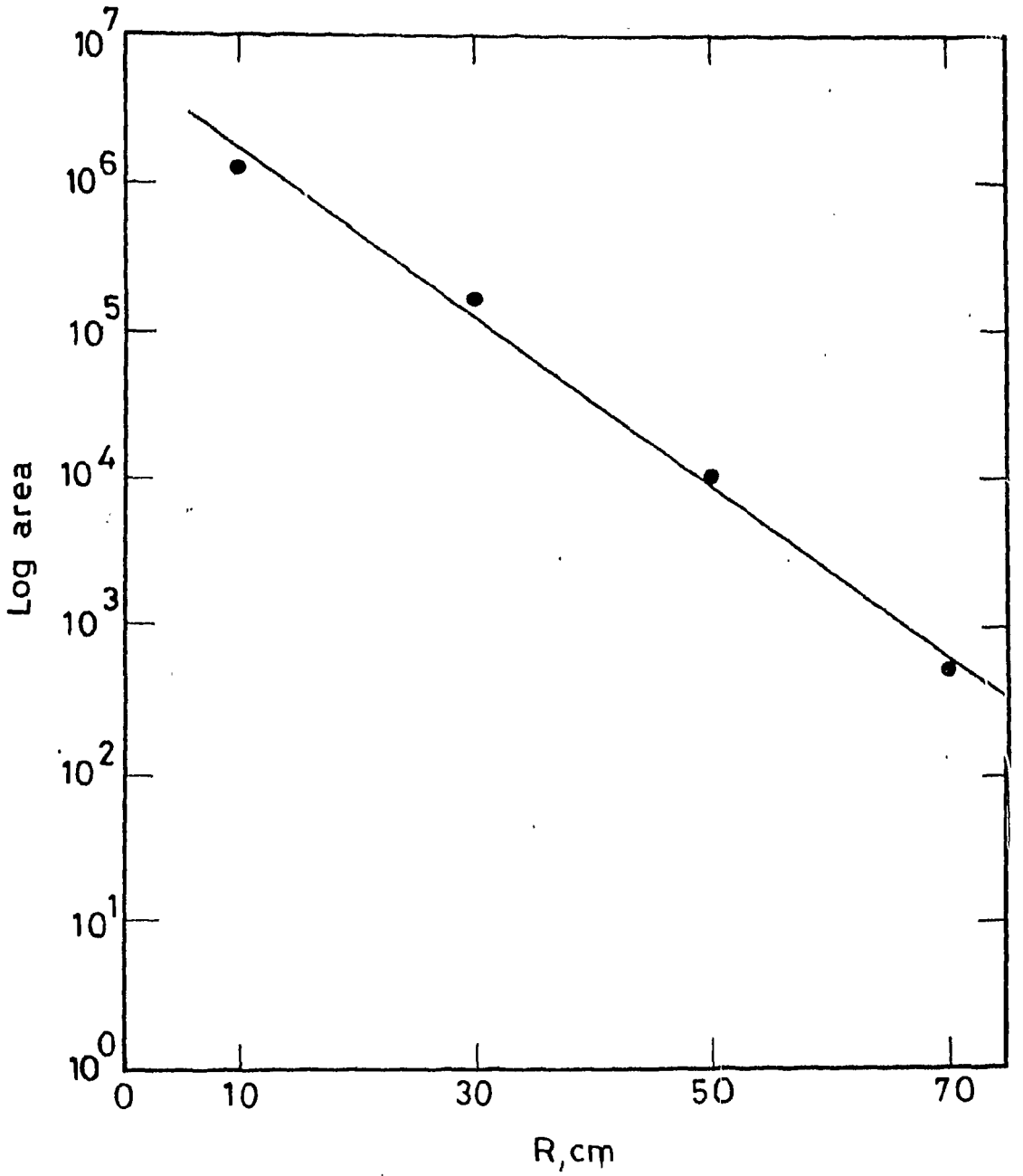

Fig.(7): Determination of the relaxation length for fast neutrons distribution in solid concrete.

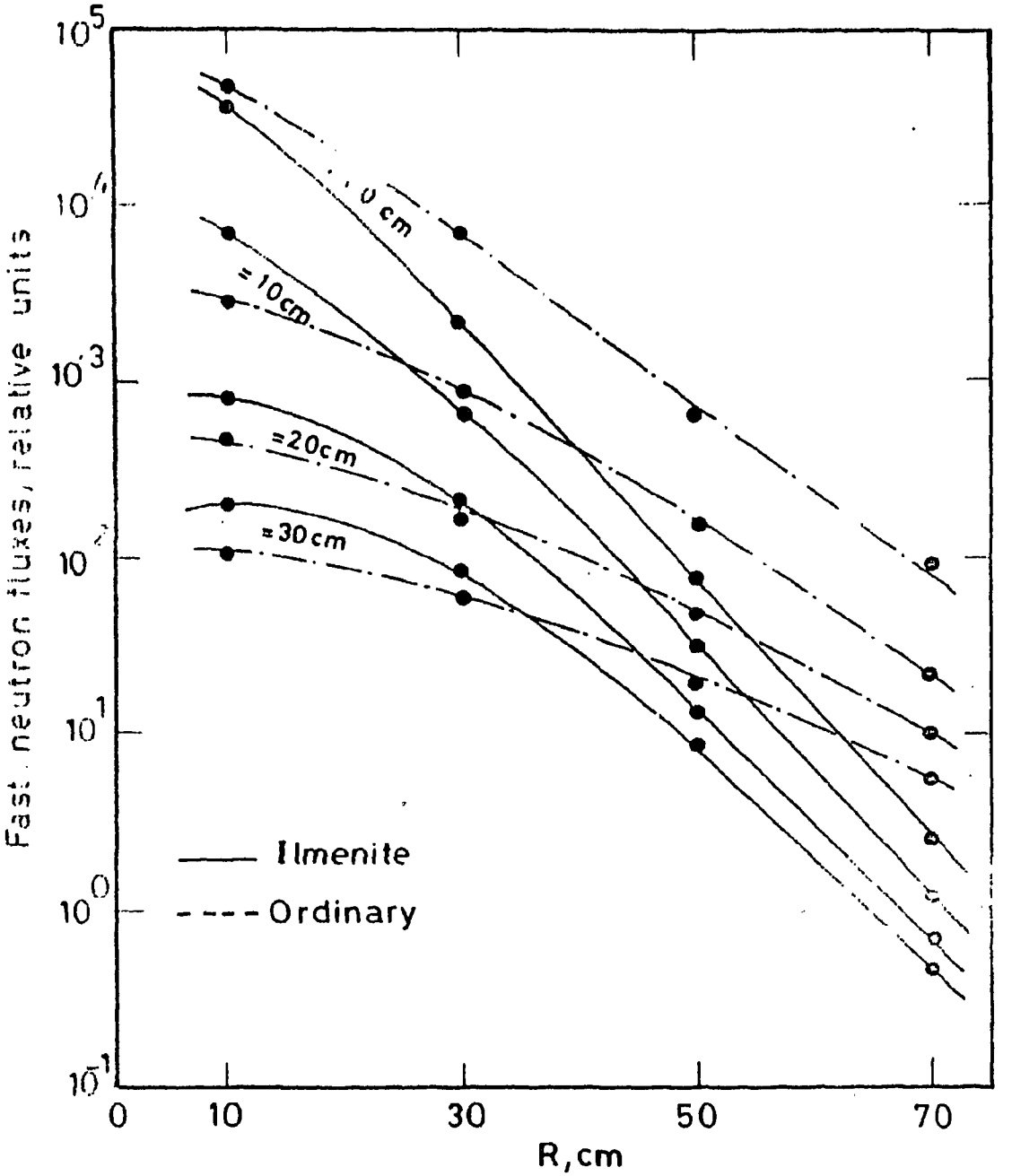

Fig.(8): Comparison between fast neutron fluxes distribution in the Egyptian ilmenite & ordinary solid concrete.

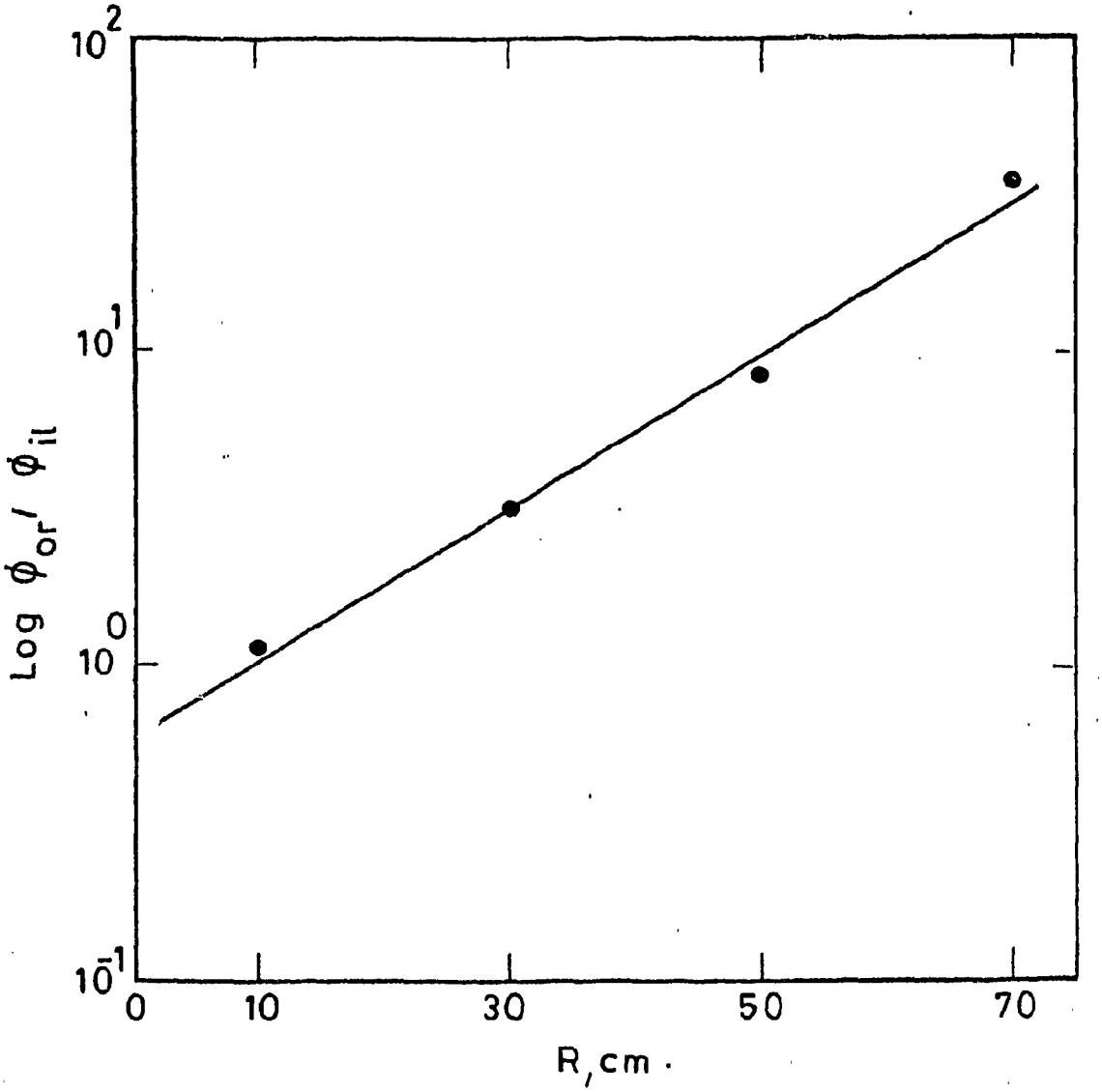

Fig.(9): Ratio between fast neutron fluxes distribution in ordinary and ilmenite concorete measured at Z = 0 cm for different values of R.